

# Adsorption and Interaction of Ethylene on RuO<sub>2</sub>(110) Surfaces<sup>†</sup>

U. A. Paulus, Y. Wang, H. P. Bonzel,<sup>‡</sup> K. Jacobi,\* and G. Ertl

Fritz-Haber-Institut der Max-Planck-Gesellschaft, Faradayweg 4-6, D-14195 Berlin, Germany

Received: March 1, 2004; In Final Form: June 17, 2004

Ethylene (C<sub>2</sub>H<sub>4</sub>) adsorbed on the stoichiometric and oxygen-rich RuO<sub>2</sub>(110) surfaces, exposing coordinatively unsaturated Ru-cus and O-cus atoms, is investigated by applying high-resolution electron energy-loss spectroscopy and thermal desorption spectroscopy in combination with isotope labeling experiments. On the stoichiometric RuO<sub>2</sub>(110) surface C<sub>2</sub>H<sub>4</sub> adsorbs and desorbs molecularly. In contrast, on the oxygen-rich RuO<sub>2</sub>(110) surface ethylene adsorbs molecularly at 85 K and is completely oxidized through interaction with O-cus and O-bridge upon annealing to 500 K. The first couple of reactions are observed at 200 K taking place on Ru-cus: A change from  $\pi$ - to  $\sigma$ -bonding, formation of  $\text{—C=O}$  and  $\text{—C—O}$  groups, and dehydrogenation giving rise to H<sub>2</sub>O adsorbed at Ru-cus. Maximum reaction rate is reached for C<sub>2</sub>H<sub>4</sub> chemisorbed at Ru-cus with O-cus neighbors on each side. A model for the first couple of reactions is sketched. For the final combustion, C<sub>2</sub>H<sub>4</sub> reacts both with O-cus and O-bridge. Ethylene oxide is not detected under any circumstance.

## 1. Introduction

Ethylene oxide is an important material for the production of several chemicals such as ethylene glycol. Silver particles dispersed on Al<sub>2</sub>O<sub>3</sub> serve as the main catalyst for the partial oxidation (epoxidation) of ethylene to ethylene oxide (compare Reference<sup>1</sup> and references therein). This reaction competes with the total oxidation to CO<sub>2</sub>. There is general agreement that both reactions—as illustrated by the scheme in Figure 1—proceed through interaction of adsorbed ethylene with atomic oxygen which indicates that also any epoxide formed may undergo total oxidation instead of desorption.

Usually one tries to apply ultrahigh vacuum (UHV) techniques to investigate basic processes of adsorption and surface reactions. However, due to the low reaction probability for ethylene oxide production on silver catalysts and the consequent requirement of high C<sub>2</sub>H<sub>4</sub> pressure, the direct reaction study under UHV conditions is considered to be unsuccessful in the case of silver catalysts.<sup>1</sup> This might be different for other surfaces.

Recently, stoichiometric and oxygen-rich RuO<sub>2</sub>(110) surfaces have been proven to be efficient CO-oxidation catalysts<sup>2,3</sup> due to their surfaces being terminated by different under-coordinated reactive oxygen atoms. In particular, the O-cus atoms (see below) of the oxygen-rich RuO<sub>2</sub>(110) surface may be regarded as electrophilic O-species,<sup>4</sup> similar to the O-species responsible for epoxidation on Ag.<sup>1</sup>

Here we study the oxidation of ethylene on the stoichiometric and oxygen-rich RuO<sub>2</sub>(110) surfaces by means of thermal desorption spectroscopy (TDS) and a vibrational spectroscopy method, here high-resolution electron energy-loss spectroscopy (HREELS). Whereas the stoichiometric surface is inactive, on the oxygen-rich surface ethylene becomes completely oxidized. First reaction steps are identified occurring at about 200 K

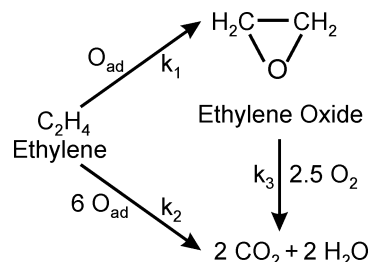


**Figure 1.** Reaction scheme for ethylene epoxidation and total oxidation.

starting from ethylene adsorbed at Ru-cus near to the neighboring O-cus. From the observed reaction intermediates a model for this first step is derived. The final complete combustion takes place at 500 K where the many anticipated reaction steps occur in a very narrow time window which is not resolvable with our methods. Epoxide could not be separated.

## 2. Experimental Section

High-resolution electron energy-loss spectroscopy (HREELS) and thermal desorption spectroscopy (TDS) were performed in a UHV apparatus, consisting of two chambers separated by a valve. The upper chamber (base pressure  $3 \times 10^{-11}$  mbar) was used for sample preparation. It was equipped with an argon ion sputtering gun, gas exposing valves, a LEED optics, and a quadrupole mass spectrometer for TDS experiments. The heating rate for TDS was approximately  $3 \text{ K s}^{-1}$ . The lower chamber (base pressure  $2 \times 10^{-11}$  mbar) housed a HREEL spectrometer of commercial Ibach design (Delta 0.5, SPECS, Germany). HREEL spectra were recorded at an angle of incidence of  $55^\circ$  with respect to the surface normal in specular geometry. The energy of the primary electrons was set to 3 eV and the spectral resolution to better than 3 meV. The substrate, a Ru(0001) single crystal, was clamped between two Ta wires. A NiCr/Ni thermocouple was spot-welded to the back of the Ru crystal. The sample temperature can be varied between 85 and  $\sim 1300$  K by combining cooling with liquid nitrogen and heating by radiation or by combined radiation and electron bombardment from the backside of the sample.

<sup>†</sup> Part of the special issue "Michel Boudart Festschrift".

\* To whom correspondence should be addressed. Telephone: ++49 30 8413 5201. Fax: ++49 30 8413 5106-3155. E-mail: jacobi@fhi-berlin.mpg.de.

<sup>‡</sup> Permanent address: Forschungszentrum Jülich, ISG3, D-52425 Jülich, Germany.

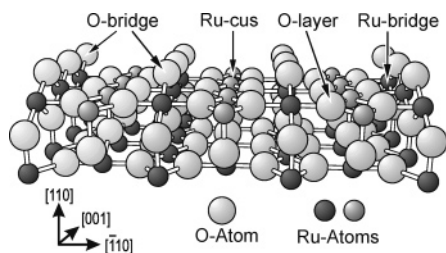


**Figure 2.** Stick-and-ball model of the stoichiometric  $\text{RuO}_2(110)$  surface.<sup>5</sup>

The  $\text{RuO}_2(110)$  surface was prepared in situ following a procedure described in preceding publications.<sup>2,5,7</sup> In short, the Ru crystal was cleaned by applying repeated sputtering and annealing cycles. The oxide was then grown epitaxially by exposing the clean  $\text{Ru}(0001)$  surface to about  $10^7$  langmuir of  $\text{O}_2$  (1 langmuir =  $1.3 \times 10^{-6}$  mbar s) at 700 K.

Prior to each experiment, impurities such as hydrogen or CO were desorbed and the surface ordering was improved by heating the sample to 700 K for 1 min. The chemical cleanliness of the surface and the surface order were controlled by standard techniques. Gases exposed to the sample surface were  $^{16}\text{O}_2$  (purity 99.998%, Messer Griesheim),  $^{18}\text{O}_2$  (min. 99 atom %  $^{18}\text{O}$ , Isotec),  $\text{C}_2\text{H}_4$  (purity 99.95%, Messer Griesheim) and  $\text{C}_2\text{D}_4$  (min. 99 atom % D, Isotec).

### 3. Results and Discussion

The structure of the stoichiometric  $\text{RuO}_2(110)$  surface is reproduced in Figure 2. The surface is composed of two types of atoms with varying coordination. The oxygen atoms are either 3-fold- or 2-fold-coordinated (O-layer and O-bridge), with the O-bridge atoms being coordinatively unsaturated. The surface Ru atoms are 5-fold coordinated and thus also coordinatively unsaturated (cus) and are called Ru-cus. The Ru atoms underneath the O-bridge atoms are 6-fold coordinated and are labeled Ru-bridge. When the stoichiometric  $\text{RuO}_2(110)$  surface was exposed to oxygen at room temperature, dissociative adsorption takes place generating O atoms adsorbed on top of the Ru-cus atoms. These oxygen atoms are in the following labeled O-cus (electrophilic species). The total coverage of O-cus depends on the oxygen exposure, with a maximum coverage of about 80% of the Ru-cus atoms being reached at an oxygen exposure of  $\geq 1.0$  langmuir.<sup>4,6</sup> The diffusion barrier for O-cus along the Ru-cus row is relatively high so that single unoccupied Ru-cus sites cannot be filled by diffusion. On the other hand dissociation of  $\text{O}_2$  needs two neighboring sites. Altogether, single unoccupied Ru-cus atoms remain which gives rise to a maximum O-cus coverage of about 0.8.

**3.1. Ethylene Adsorption on the Stoichiometric  $\text{RuO}_2(110)$  Surface. 3.1.1. Thermal Desorption Spectra of  $\text{C}_2\text{H}_4$  Adsorbed on Stoichiometric  $\text{RuO}_2(110)$ .** Parts a and b of Figure 3 present the TD-spectra obtained after exposing the stoichiometric  $\text{RuO}_2(110)$  surface to 0.6 langmuir of  $\text{C}_2\text{H}_4$  and  $\text{C}_2\text{D}_4$ , respectively. Desorption peaks are observed at masses 28 ( $\text{C}_2\text{H}_4$ ), 27 ( $\text{C}_2\text{H}_3$ ), 26 ( $\text{C}_2\text{H}_2$ ), and 14 ( $\text{CH}_2$ ) at 155 ( $\alpha$ ), 240 ( $\beta$ ), and 320 K ( $\gamma$ ). The relative intensities of these mass signals closely resemble the cracking pattern of  $\text{C}_2\text{H}_4$ . For  $\text{C}_2\text{D}_4$ , equivalent signals are observed at masses 32 ( $\text{C}_2\text{D}_4$ ), 30 ( $\text{C}_2\text{D}_3$ ), 28 ( $\text{C}_2\text{D}_2$ ), and 16 ( $\text{CD}_2$ ). These observations demonstrate that ethylene adsorbs and desorbs molecularly. Integration of the intensities below the three desorption peaks reveals that about 70% of the adsorbed ethylene desorbs in the  $\gamma$  state at 320 K. Because of the background pressure of  $\text{H}_2$  and  $\text{H}_2\text{O}$ , the  $\text{H}_2$  signal is very noisy and is not presented here. The small amount of  $\text{D}_2$  (mass

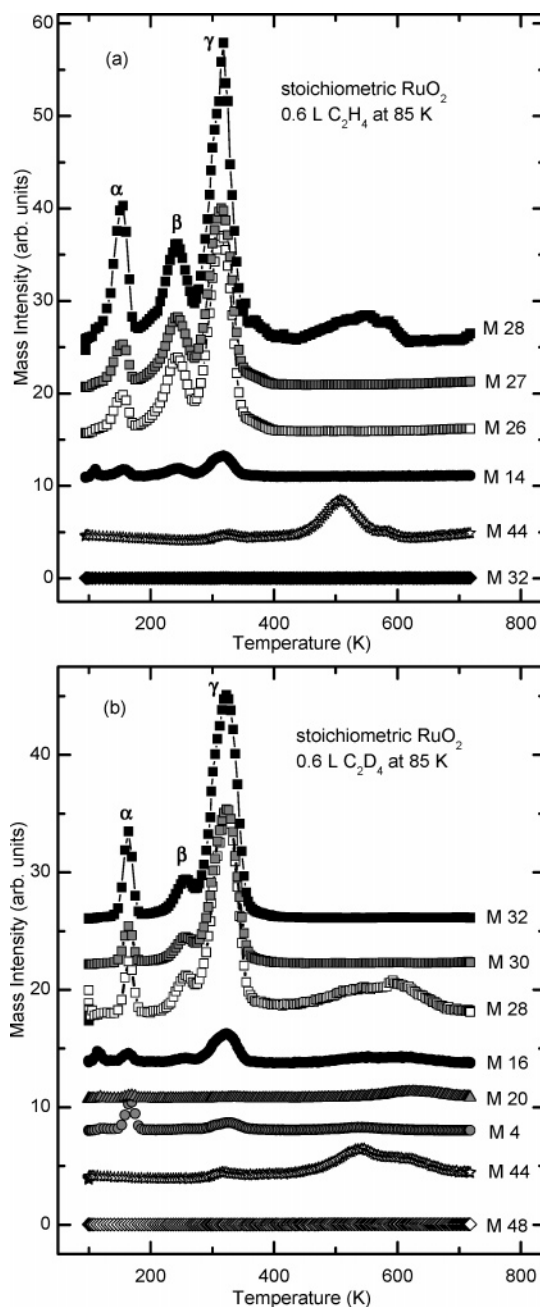


**Figure 3.** (a) TD spectra obtained after exposing 0.6 langmuir of  $\text{C}_2\text{H}_4$  to the stoichiometric  $\text{RuO}_2(110)$  surface at 85 K. (b) TD spectra obtained after exposing 0.6 langmuir of  $\text{C}_2\text{D}_4$  to the stoichiometric  $\text{RuO}_2(110)$  surface at 85 K. The corresponding masses are indicated.

4) detected at 165 and 320 K is likely to be due to some coadsorption.

A small fraction of mass 28 is observed at  $\sim 550$  K, both for  $\text{C}_2\text{H}_4$  and  $\text{C}_2\text{D}_4$ , and is accompanied by mass 44 and mass 16 signals which are typical for  $\text{CO}_2$ . The high desorption temperature of this  $\text{CO}_2$  indicates desorption directly after its formation.<sup>8</sup> Ethylene oxide ( $\text{C}_2\text{H}_4\text{O}$ , mass 44) can be ruled out as source of the mass 44 channel: First of all, it desorbs below room temperature.<sup>9</sup> Furthermore, mass 44 is detected at the same temperature and with similar intensity after exposing  $\text{C}_2\text{D}_4$ , whereas no mass 48 ( $\text{C}_2\text{D}_4\text{O}$ ) is observed. Finally, the mass 44 signal intensity is independent of the ethylene exposure (not shown). Thus, background adsorption of CO, followed by reaction with O-bridge forming  $\text{CO}_2$ , can be assumed as its source.

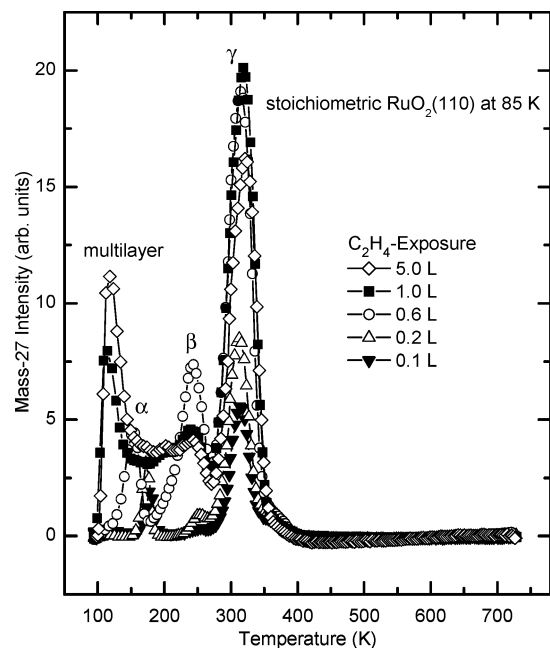


**Figure 4.** Mass-27 signal ( $C_2H_3$ -fragment from the mass spectrometer cracking pattern of  $C_2H_4$ ) after exposing  $C_2H_4$  to the stoichiometric  $RuO_2(110)$  surface at 85 K. The exposure values are given in units of langmuir (1 langmuir =  $1.33 \times 10^{-6}$  mbar s).

A  $H_2O$  signal (mass 18, not shown) is also independent of the  $C_2H_4$  exposure. As upon  $C_2D_4$  adsorption only small amounts of  $D_2O$  (mass 20) but similar amounts of  $H_2O$  are observed,  $H_2$  adsorption from the background and its interaction with O-bridge<sup>10</sup> are made responsible for the  $H_2O$  formation. The lack of considerable  $D_2O$  formation on the stoichiometric surface clearly confirms that total combustion of ethylene is not taking place.

Figure 4 presents the ethylene desorption signal after varying the  $C_2H_4$  exposure. (To avoid contributions from CO, mass 27 is plotted here.) For 0.1 langmuir of  $C_2H_4$  exposure the main desorption peak ( $\gamma$  peak) is observed at  $\sim 320$  K. With increasing  $C_2H_4$  exposure, the  $\gamma$  peak saturates while the  $\alpha$  peak at  $\sim 155$  K and the  $\beta$  peak at  $\sim 240$  K emerge. The final stage—with a sharp peak at  $\sim 110$  K and the  $\alpha$  and  $\beta$  peaks merging into one broad band between 150 and 250 K—is reached at around 1.0 langmuir. The peak at  $\sim 110$  K increases in intensity with further  $C_2H_4$  exposure and slightly shifts to higher temperature indicating zero-order desorption kinetics. Therefore, it is attributed to desorption of multilayer  $C_2H_4$ . We attribute hence the  $\gamma$  peak at 320 K to  $C_2H_4$  adsorbed on the stoichiometric  $RuO_2(110)$  surface and the peak at 110 K to multilayer  $C_2H_4$ , while the  $\alpha$  and  $\beta$  states are likely due to lateral repulsive interaction. The portion of  $\alpha$  and  $\beta$  states is too large to be assigned to defect sites.

**3.1.2. HREELS of  $C_2H_4$  Adsorbed on Stoichiometric  $RuO_2(110)$ .** The following results obtained by HREELS characterize the adsorbed ethylene layer under various conditions. Spectrum a in Figure 5 is characteristic for the clean, stoichiometric  $RuO_2(110)$  surface, with phonon contributions at 12 and 45 meV and the O-bridge vibration perpendicular to the surface at 69 meV.<sup>2,4,7</sup> Spectra b and c were recorded after exposing this surface at 85 K to 0.6 langmuir of  $C_2H_4$  and  $C_2D_4$ , respectively. Additional signals are observed at 57, 126, 150, 164, 171, 194, and 230 meV and two doublets at 371/382, and 433/447 meV. The signals at 57, 230, and 433/447 meV are observed quite often, when analyzing  $RuO_2(110)$  surfaces at

low temperatures, and are assigned to the translation, scissoring, and stretching modes of  $H_2O_{bridge}$  groups.<sup>10,11</sup> Their origin is background adsorption of  $H_2$  on O-bridge.<sup>10</sup> The doublet at 371/382 meV observed in spectrum b shifts to 277/287 meV upon  $C_2D_4$  exposure and is assigned, therefore, to the symmetric and asymmetric C—H (C—D) stretch vibrations.

The weakening of the O-bridge peak at 69 meV (Figure 5, spectra b and c) can be due to shielding from  $C_2H_4$  ( $C_2D_4$ ) and/or due to formation of  $H_2O$ . The latter aspect could explain, why in the case of an  $O_{cus}$ -precovered surface, where fewer  $H_2O/OH$  groups are formed, the signals for O-bridge and O-cus remain unaffected upon  $C_2H_4$  ( $C_2D_4$ ) exposure (Figure 5, spectra d and e, which will be discussed in section 3.2 below).

When the presented HREEL spectra are compared to those obtained for  $C_2H_4$  on  $Ru(0001)$ ,<sup>12,13</sup> the peak at 194 meV is identified as the  $\nu(C=C)$  stretching mode what is supported by the isotope shift of 1.08 (shift to 180 meV upon exposing  $C_2D_4$ ). It appears at a rather high energy, indicating a fairly strong C=C bond, which is nearly unperturbed relative to the gas phase.<sup>12</sup> Consequently, the adsorption is only rather weak. In agreement with the conclusions in reference 14 and by Stuve and Madix for O-covered surfaces,<sup>15</sup> adsorption in a  $\pi$ -configuration is assumed. The most intensive loss of  $C_2H_4$  ( $C_2D_4$ , isotope shift) lies at 126 meV (94 meV, 1.34) (note the different sensitivity factors  $\times 50$  and  $\times 100$  in Figure 5) and is attributed to the wagging mode. This assignment is in line with the suggested  $\pi$ -configuration where the C=C is oriented parallel to the surface. On  $Ru(0001)$  the wagging mode at 120 meV was found to be the most intense signal for weakly  $\pi$ -bonded (multilayer) ethylene.<sup>12</sup> Less-intense losses are found at 150 meV (112 meV, 1.34), 164 meV (122 meV, 1.34), and 171 meV (131 meV, 1.31). These modes correspond to the rocking, twisting, and scissoring modes.

**3.1.3. Thermally Activated Transformation of  $C_2H_4$  on Stoichiometric  $RuO_2(110)$ .** Further insight into thermally activated transformations of the ethylene adsorbed on Ru-cus was obtained through variation of the temperature. When heated to 200 K, no spectral changes occur. Figure 6 presents HREEL spectra obtained after heating to 260 K (spectra a and b) and 400 K (spectra c and d), respectively. After the sample was heated to 260 K, a temperature which lies between the  $\beta$  and  $\gamma$  peaks in TDS (see Figure 3), spectra a and b clearly differ from those recorded directly after exposure at 85 K (compare Figure 5, spectra b and c). The C—H stretch vibration signals shift from 371/382 to 354/360 meV for  $C_2H_4$ . For  $C_2D_4$  the doublet is better resolved at 263/273 meV. The existence of a doublet in the C—H stretch region together with the first-order ethylene desorption observed in TDS at 320 K indicates that molecular ethylene must still be present on the surface. Thus, a likely explanation for the changes in the spectra, especially for the shift of the C—H stretch vibration signal to lower energy—indicating a weakening of the C—H bond—is a change in adsorption strength of the  $C_2H_4$ . The peak at 194 (180) meV disappeared and a new peak appeared at 144 (136) meV. From comparison with ethylene  $\sigma$ -bonded to  $Ru(0001)$ ,<sup>12</sup> we assign the signal at 144 meV (136 meV, 1.06) to the stretch vibration of the single C—C bond as further confirmed by the calculations made by Stacchiola et al.<sup>17</sup> We suggest therefore a conversion from  $\pi$ -bonded to  $\sigma$ -bonded ethylene which was also observed for ethylene adsorbed on a  $Pt(111)/O$  surface.<sup>18</sup>

An unambiguous assignment of the vibrational signals for the wagging, rocking, twisting, and scissoring modes between 100 and 200 meV is more difficult, but clear shifts to higher energies are observed after annealing: 126  $\rightarrow$  133, 150  $\rightarrow$  157;

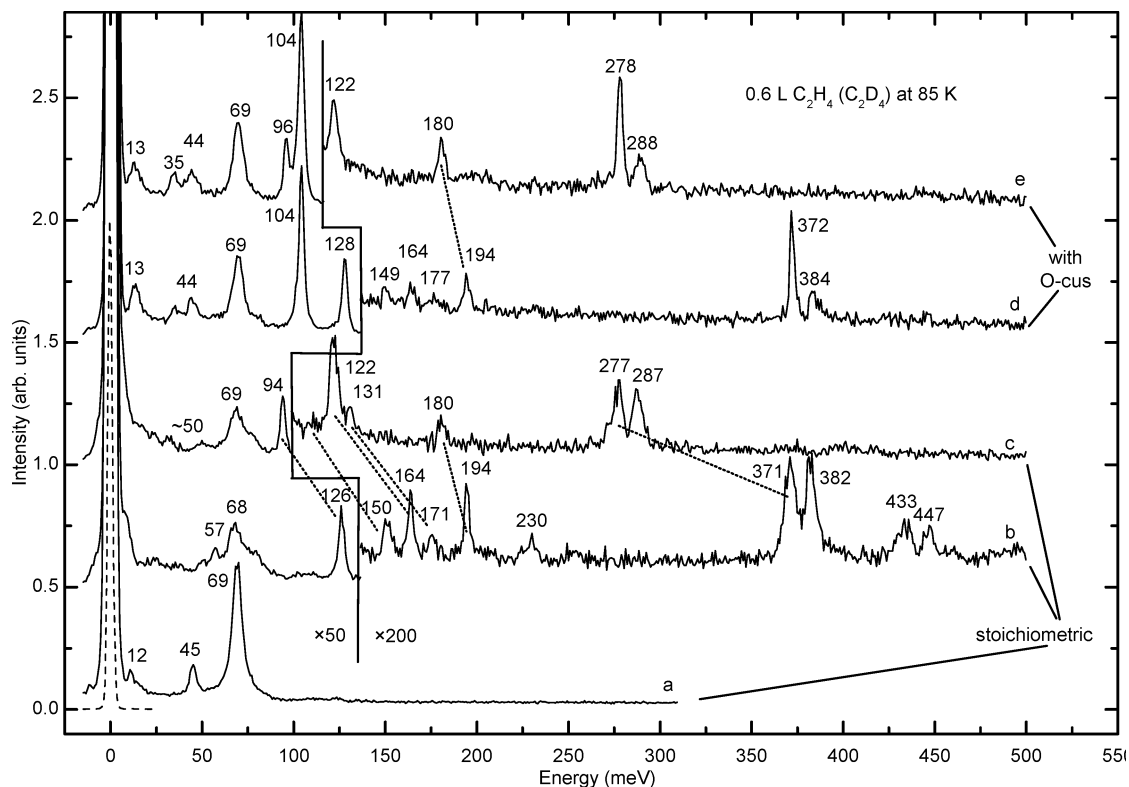


**Figure 5.** HREEL spectra of the stoichiometric  $\text{RuO}_2(110)$  surface: (a) recorded at 300 K; (b) after exposing 0.6 langmuir of  $\text{C}_2\text{H}_4$ , recorded at 85 K; (c) after exposing 0.6 langmuir of  $\text{C}_2\text{D}_4$ , recorded at 85 K; (d) after preparing an oxygen saturated surface (exposing 1.0 langmuir of  $\text{O}_2$  at 300 K) and subsequently exposing 0.6 langmuir of  $\text{C}_2\text{H}_4$ , recorded at 85 K; (e) after preparing an oxygen saturated surface (exposing 1.0 langmuir of  $\text{O}_2$  at 300 K) and subsequently exposing 0.6 langmuir of  $\text{C}_2\text{D}_4$ , recorded at 85 K.

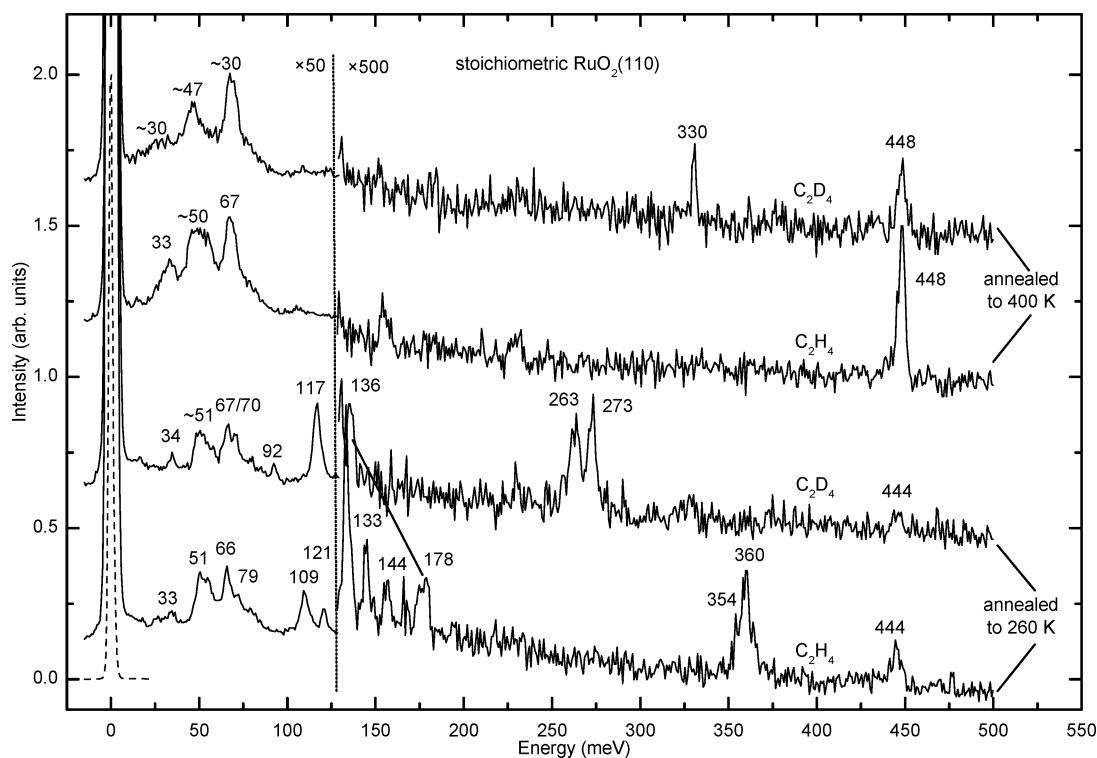


**Figure 6.** HREEL spectra of the stoichiometric  $\text{RuO}_2(110)$  surface recorded at 85 K: (a) after exposing 0.6 langmuir of  $\text{C}_2\text{H}_4$  at 85 K and subsequently annealing to 260 K; (b) after exposing 0.6 langmuir of  $\text{C}_2\text{D}_4$  at 85 K and subsequently annealing to 260 K for 30 s; (c and d) same as parts a and b but annealing to 400 K.<sup>11</sup>

164  $\rightarrow$  167; 171  $\rightarrow$  178 (all values in meV). Obviously and reasonably, the anticipated wagging mode at 133 meV is no longer of high intensity. All shifts are induced by the change from  $\pi$ - to  $\sigma$ -bonding.

After the sample was heated to 400 K, the spectra look nearly identical for both  $\text{C}_2\text{H}_4$  (spectrum c) and  $\text{C}_2\text{D}_4$  (spectrum d). The signals at  $\sim 30$ , 50, and 448 meV present in both spectra are attributed to  $\text{O}_{\text{bridge}}\text{H}$ .<sup>10</sup> The only difference is a signal at



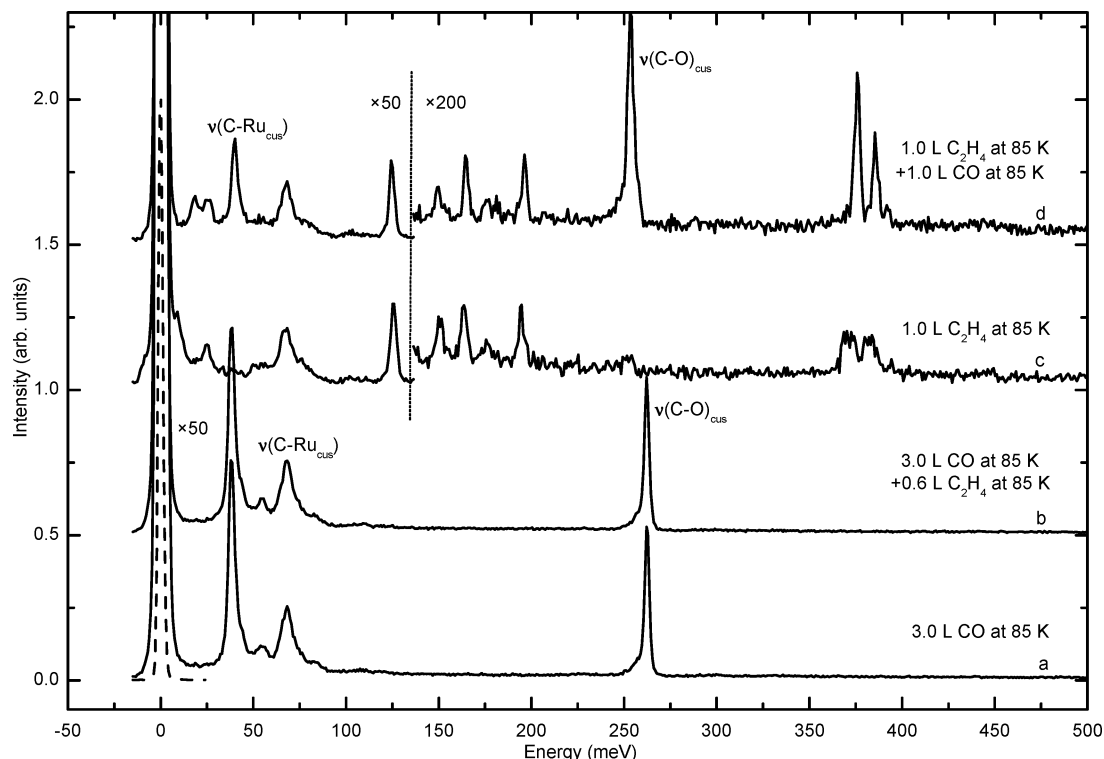


**Figure 7.** HREEL spectra of the stoichiometric RuO<sub>2</sub>(110) surface: (a) after exposing 3.0 langmuir of CO at 85 K; (b) after exposing 3.0 langmuir of CO at 85 K and subsequently exposing 0.6 langmuir of C<sub>2</sub>H<sub>4</sub> at 85 K; (c) after exposing 1.0 langmuir of C<sub>2</sub>H<sub>4</sub> at 85 K; (d) after exposing 1.0 langmuir of C<sub>2</sub>H<sub>4</sub> at 85 K and subsequently exposing 1.0 langmuir of CO at 85 K.

330 meV due to some traces of surface OD groups which is consistent with traces of D<sub>2</sub>O detected during TDS.

**3.1.4. Adsorption Site of Ethylene on Stoichiometric RuO<sub>2</sub>(110).** To elucidate the adsorption sites of ethylene, the following two experiments were performed: Spectrum a of Figure 7 was taken after the stoichiometric RuO<sub>2</sub>(110) surface was exposed to 3 langmuir of CO at 85 K.

From previous studies, we know<sup>7</sup> that CO-cus adsorbs on top of Ru-cus at 85 K with the signal at 39 meV corresponding to the C–Ru<sub>cus</sub> stretch vibration and the signal at 262 meV to the C–O stretch vibration. At 3.0 langmuir of CO, about 100% occupation is reached.<sup>16</sup> Spectrum b of Figure 7 was taken after the stoichiometric surface was exposed to 3.0 langmuir of CO at 85 K, followed by 0.6 langmuir of C<sub>2</sub>H<sub>4</sub> at 85 K. Obviously, spectrum b does not change—compared to spectrum a—upon exposing C<sub>2</sub>H<sub>4</sub>; i.e., adsorption of C<sub>2</sub>H<sub>4</sub> does not take place. From this experiment, it has to be concluded that ethylene does adsorb neither on top of O-bridge nor on top of CO the latter being adsorbed at Ru-cus. We performed an additional experiment in which we saturated the surface with O-cus at room temperature and blocked the remaining 20% empty Ru-cus sites by adsorption of CO at 85 K. Also in this case no additional ethylene could be adsorbed. This shows that ethylene is also not adsorbed on top of O-cus. Thus, it has to be concluded that free Ru-cus sites are the prerequisite for C<sub>2</sub>H<sub>4</sub> adsorption. Consequently, in the case of the oxygen-saturated surface discussed below, only the remaining ~20% empty Ru-cus sites adsorb C<sub>2</sub>H<sub>4</sub>.

Spectrum c of Figure 7 was taken after the same stoichiometric surface was exposed to 1.0 langmuir of C<sub>2</sub>H<sub>4</sub> at 85 K. The signals for  $\pi$ -bonded C<sub>2</sub>H<sub>4</sub> described above are clearly visible. Spectrum d is obtained after subsequently exposing 1.0 langmuir of CO at 85 K. Besides the signals for  $\pi$ -bonded C<sub>2</sub>H<sub>4</sub>, the Ru–C and C–O stretch vibrations of CO-cus are visible. This demonstrates that even at C<sub>2</sub>H<sub>4</sub> saturation still free Ru-

cus sites (“holes in the C<sub>2</sub>H<sub>4</sub> packing”) are available allowing the coadsorption of CO. The redshift for  $\nu$ (C–O)-cus to 252 meV is attributed to interactions between neighboring CO and C<sub>2</sub>H<sub>4</sub> species: The electron density of the substrate, increased by adsorbed C<sub>2</sub>H<sub>4</sub>—as reflected by a decrease of the work function—will enhance the electron back-donation into the 2 $\pi^*$  antibonding orbital of the CO molecule, especially for low CO coverage, resulting in a strengthening of the Ru–CO bond together with a weakening of the internal C–O bond.

**3.2. Ethylene Adsorption on the O-rich RuO<sub>2</sub>(110) Surface.** The oxygen-rich RuO<sub>2</sub>(110) surface is prepared by exposing the stoichiometric RuO<sub>2</sub>(110) surface to 1.0 langmuir of O<sub>2</sub> at room temperature, leading to a high coverage of O-cus (about 80% of all Ru-cus sites are occupied by O-cus).

**3.2.1. Thermal Desorption Spectroscopy of C<sub>2</sub>H<sub>4</sub> on O-Rich RuO<sub>2</sub>(110).** Parts a and b of Figure 8 present the TD spectra obtained after exposing this surface to 0.6 langmuir of C<sub>2</sub>H<sub>4</sub> or C<sub>2</sub>D<sub>4</sub> at 85 K. At 120, 400, and 500 K, strong desorption signals are found. Unlike for the stoichiometric surface, desorption signals for mass 44, mass 28, and mass 16 are observed at 500 K with similar intensities for both C<sub>2</sub>H<sub>4</sub> and C<sub>2</sub>D<sub>4</sub> exposures. The intensity ratios of these three mass signals resemble closely the cracking pattern of CO<sub>2</sub>. No desorption of chemisorbed C<sub>2</sub>H<sub>4</sub> or C<sub>2</sub>D<sub>4</sub> is detected and no O<sub>2</sub> desorption is observed. These observations clearly demonstrate that the entire adsorbed ethylene population has reacted with oxygen and that a complete conversion to CO<sub>2</sub> (and H<sub>2</sub>O as discussed below) has taken place. All O-cus species have been reacted off. The high desorption temperature of CO<sub>2</sub> indicates that release of CO<sub>2</sub> into the gas phase parallels its formation. The sharp peaks observed around 120 K for the masses 28, 27, and 26 (C<sub>2</sub>H<sub>4</sub>) and the masses 32, 30, and 28 (C<sub>2</sub>D<sub>4</sub>) are attributed to multilayer ethylene, as before.

The observation of H<sub>2</sub>O (mass 18) and D<sub>2</sub>O (mass 20) signals is in agreement with the complete oxidation of ethylene to CO<sub>2</sub>

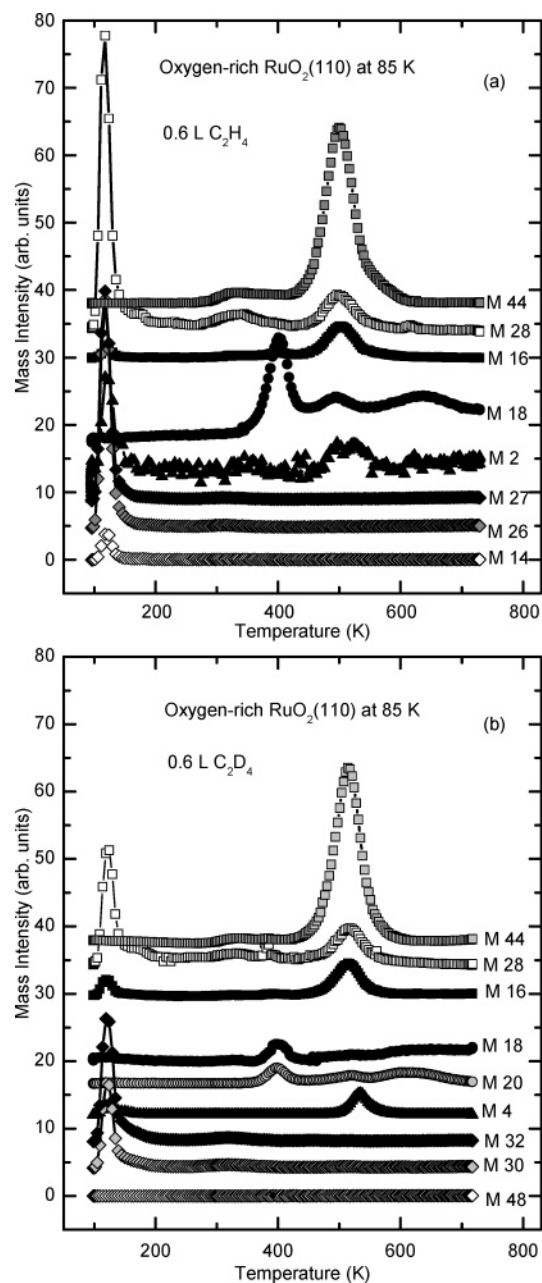
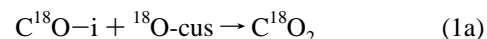


**Figure 8.** (a) TD spectra for oxygen-rich (1.0 langmuir of  $^{16}\text{O}_2$  at 300 K)  $\text{RuO}_2(110)$  surface after exposing 0.6 langmuir of  $\text{C}_2\text{H}_4$  at 85 K. (b) Same as part a but after exposing 0.6 langmuir of  $\text{C}_2\text{D}_4$ . The corresponding masses are indicated.

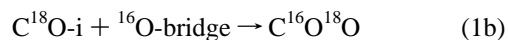
and  $\text{H}_2\text{O} \cdot \text{H}_2\text{O}$  ( $\text{D}_2\text{O}$ ) desorption proceeds in three steps: (1) A sharp desorption peak is centered around 400 K. This peak is attributed to the molecular desorption of water from the Ru-cus sites<sup>19</sup> and contains some contribution from the residual gas because, following exposure to  $\text{C}_2\text{D}_4$  (Figure 8b), one can discriminate between  $\text{H}_2\text{O}$  from the background and  $\text{D}_2\text{O}$  from the reaction of  $\text{D}_2\text{H}_4$ . (2) A second peak is observed at around 500 K, i.e., accompanying the  $\text{CO}_2$  desorption. Interestingly, when  $\text{C}_2\text{D}_4$  (Figure 8b) is exposed, the peak at 500 K is only visible for mass 20 ( $\text{D}_2\text{O}$ ) but not for mass 18 ( $\text{H}_2\text{O}$ ). Furthermore, this peak occurs only, when O-cus was present and a significant  $\text{CO}_2$  desorption (i.e., total combustion of ethylene) takes place. We conclude that the peak at 500 K originates from the desorption of  $\text{H}_2\text{O}$  formed upon the dehydrogenation of ethylene. Furthermore, this  $\text{H}_2\text{O}$  is formed by interaction with O-bridge as discussed below. Some molec-

ular  $\text{H}_2(\text{D}_2)$  desorption also accompanies the  $\text{CO}_2$  and  $\text{H}_2\text{O}$  desorption at  $\sim 500$  K. (3) A broad peak in the temperature range between 500 and 700 K is attributed to the desorption of water, following disproportionation of OH (OD) from the Ru-bridge sites in accordance with known data.<sup>10</sup> Hydroxyl groups can form via reactions of O-bridge with background  $\text{H}_2$ , spurious amounts of  $\text{H}_2$  ( $\text{D}_2$ ) in the ethylene during exposure, or hydrogen from decomposition of ethylene. No  $\text{C}_2\text{D}_4\text{O}$  is detected in the whole temperature range, demonstrating the complete lack of ethylene oxide formation.

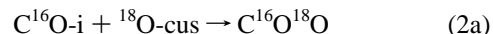
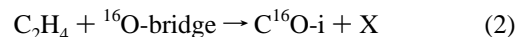
Concerning the details of the formation of  $\text{CO}_2$  from a reaction of  $\text{C}_2\text{H}_4$  with O-cus or O-bridge, the oxygen-rich  $\text{RuO}_2(110)$  surface was prepared by exposure to either  $^{16}\text{O}$  or  $^{18}\text{O}$ . Since the stoichiometric  $\text{RuO}_2(110)$  surface is always prepared with  $^{16}\text{O}$ , the O-bridge is always an  $^{16}\text{O}$  species. However, the O-cus may be either  $^{16}\text{O}$  or  $^{18}\text{O}$  depending on the additional oxygen exposure. Hence one can in principle think of the following reaction pathways where X stands for the other unspecified products of the reaction:



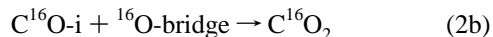
cracking pattern: 48–30–18



cracking pattern: 46–30–28–18–16



cracking pattern: 46–30–28–18–16



cracking pattern: 44–28–16

To differentiate between these reaction pathways, the following isotope-labeling experiments were performed: The stoichiometric  $\text{RuO}_2(110)$  surface was exposed to 0.1, 0.4, and 1 langmuir of  $^{18}\text{O}_2$  at room temperature—resulting in a surface terminated by  $^{16}\text{O}$ -bridge and  $^{18}\text{O}$ -cus—prior to exposing 0.6 langmuir of  $\text{C}_2\text{H}_4$  at 85 K. Figure 9 shows the corresponding TD signals for the case of 1.0 langmuir of  $^{18}\text{O}_2$ . The weak signal from mass 28—for temperatures above 150 K—indicates that only minor amounts of monolayer  $\text{C}_2\text{H}_4$  desorb molecularly. The signals for all three possible  $\text{CO}_2$  species, i.e., mass 48, 46, and 44, are clearly visible in the spectrum. The relative intensity ratios of the different  $\text{CO}_2$  species obtained when applying different  $^{18}\text{O}$ -cus coverage are listed in Table 1. For low  $^{18}\text{O}$ -cus coverage  $\text{C}^{16}\text{O}_2$  and  $\text{C}^{16}\text{O}^{18}\text{O}$  are the main products—besides molecular ethylene desorption—whereas  $\text{C}^{18}\text{O}_2$  resulting from a reaction with two  $^{18}\text{O}$ -cus species is only present as a trace. With increasing  $^{18}\text{O}$ -cus coverage, molecular ethylene desorption as well as the amount  $\text{C}^{16}\text{O}_2$  resulting from pure reaction of a C fragment with  $^{16}\text{O}$ -bridge decreases rapidly, and  $\text{C}^{18}\text{O}_2$  becomes the main desorption product. Thus, both reaction pathways 1 and 2 are confirmed. This observation, together with the finding that molecular ethylene desorption is suppressed once sufficient O-cus is present, strongly suggests that O-cus initiates the ethylene combustion. Probable at least one C atom of ethylene interacts with O-cus (pathway 1) whereas, depending on the total O-cus coverage, the second C atom may interact either with an additional O-cus (pathway 1) or with a nearby O-bridge (pathway 2).

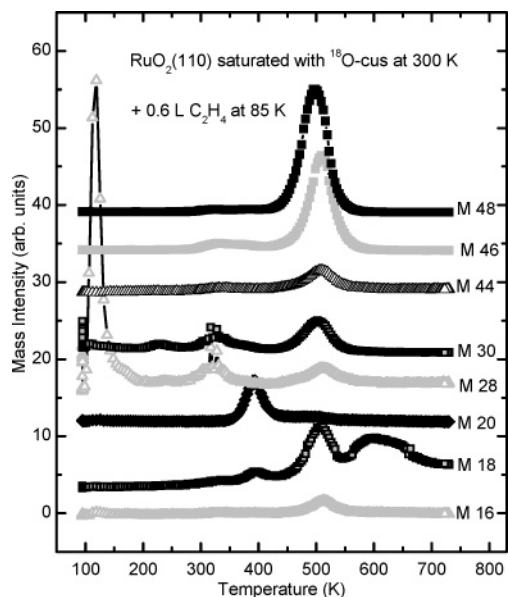


**Figure 9.** TD spectra for oxygen-rich RuO<sub>2</sub>(110) surface after exposing 1.0 langmuir of <sup>18</sup>O<sub>2</sub> to the stoichiometric RuO<sub>2</sub>(110) surface at 300 K and subsequently exposing 0.6 langmuir of C<sub>2</sub>H<sub>4</sub> at 85 K. The detected masses are indicated.

**TABLE 1: Comparison of the Ratio of the Three Different Carbon Dioxide Species, C<sup>16</sup>O<sub>2</sub>, C<sup>16</sup>O<sup>18</sup>O, and C<sup>18</sup>O<sub>2</sub>, Produced during Total Combustion of Ethylene for Different Initial <sup>18</sup>O-cus Coverage<sup>a</sup>**

<sup>18</sup> O <sub>2</sub> -exposure, langmuir	% C <sup>16</sup> O <sub>2</sub>	% C <sup>16</sup> O <sup>18</sup> O	% C <sup>18</sup> O <sub>2</sub>
0.1	44	47	9
0.4	23	51	26
1.0	9	40	51

<sup>a</sup> <sup>16</sup>O is always supplied by the O-bridge of the stoichiometric crystal.

Interestingly, the strong H<sub>2</sub><sup>18</sup>O peak (mass 20) at 400 K in Figure 9 demonstrates that H<sub>2</sub>O formation is a competing reaction for the consumption of O-cus. The desorption at 400 K is to about 90% due to dehydrogenation of C<sub>2</sub>H<sub>4</sub> leading to H<sub>2</sub><sup>18</sup>O<sub>cus</sub> and is not connected to previously adsorbed background H<sub>2</sub><sup>16</sup>O. On the other hand, the H<sub>2</sub><sup>16</sup>O peak (mass 18) at 500 K is only from the reaction of fragments (as source of hydrogen) with O-bridge, since <sup>16</sup>O is available only as O-bridge, and at 500 K no H<sub>2</sub>O release from background reactions is observed.

In summarizing the TDS results, the following important conclusion can be drawn: The presence of O-cus is essential for initiating complete oxidation of ethylene on RuO<sub>2</sub>(110). Nonetheless, O-bridge is also involved in this process. This conclusion is quite obvious already from the simple gross reaction (see Figure 1): For the complete combustion of C<sub>2</sub>H<sub>4</sub> six oxygen atoms are necessary, whereby on average only four of them are supplied by the O-cus atoms because of the 80% saturation coverage for O-cus. (For a 80% coverage of O-cus we have one adsorption site for C<sub>2</sub>H<sub>4</sub> for every four O-cus atoms.) Hence, interactions are taking place between O-cus as well as O-bridge with ethylene, ethylene intermediates, and fragments, which should manifest themselves also in the HREELS data.

**3.2.2. HREELS of C<sub>2</sub>H<sub>4</sub> on O-Rich RuO<sub>2</sub>(110) for the Reaction at 200 K.** Returning to Figure 5, we now discuss the vibrational spectra d and e recorded after exposing the O-rich RuO<sub>2</sub>(110) surface at 85 K to 0.6 langmuir of C<sub>2</sub>H<sub>4</sub> (d) and C<sub>2</sub>D<sub>4</sub> (e), respectively. Apart from some slight variations concerning peak positions and intensities, the spectra are

practically identical to those recorded from the stoichiometric RuO<sub>2</sub>(110) surface, reproduced in spectra b and c, except that the signal at 104 meV in spectra d and e is due to the O-cus stretch vibration perpendicular to the surface. The intensity of the O<sub>cus</sub>-specific peak is hardly effected by adsorbed C<sub>2</sub>H<sub>4</sub> at 85 K which indicates that C<sub>2</sub>H<sub>4</sub> does not adsorb on top of O<sub>cus</sub>. We conclude that ethylene is adsorbed on the remaining (~20%) oxygen-free Ru-cus sites. Hence, again a rather weak  $\pi$ -type adsorption of ethylene is concluded for this surface at 85 K.

From TDS, we have already derived, that total combustion of ethylene takes place upon heating to 500 K. Besides CO<sub>2</sub> and H<sub>2</sub>O, no other desorbing species could be detected. Upon ethylene exposure and subsequent stepwise heating, one can think of a number of processes taking place on the oxygen saturated RuO<sub>2</sub>(110) surface through the interaction of ethylene with Ru-cus, O-cus, and O-bridge: (i) rearrangement of H atoms of ethylene including the formation of CH- and CH<sub>3</sub>-groups; (ii) dehydrogenation leading to the formation of OH/H<sub>2</sub>O-groups as well as C–O bonds; (iii) fragmentation, i.e., breaking of the C–C bonds. The HREELS data recorded after stepwise heating reveal indeed a rather complex picture reflecting such kinds of transformations.

Figure 10 presents the vibrational spectra following stepwise annealing of the ethylene adlayer on oxygen-rich RuO<sub>2</sub>(110) to 250 and 360 K, respectively. When the reaction was heated to 250 K, both the Ru–O<sub>bridge</sub> and the Ru–O<sub>cus</sub> stretch vibrations at 69 and 104 meV, are still clearly resolved. (Note that the Ru–<sup>18</sup>O<sub>cus</sub> signal is shifted to 99 meV from 104 meV for Ru–<sup>16</sup>O<sub>cus</sub>.) However, a strong weakening of the O-cus signal is observed compared to spectra d and e in Figure 5 taken directly after exposing at 85 K. In addition, a couple of other changes are observed.

As we expected the formation of C–O bonds, we performed isotope labeling experiments using <sup>16</sup>O and <sup>18</sup>O. In Figure 10, we first compare the spectra obtained for O-rich (80% O-cus) surfaces prepared by using <sup>16</sup>O<sub>2</sub> and <sup>18</sup>O<sub>2</sub> and subsequent exposure to C<sub>2</sub>H<sub>4</sub> or C<sub>2</sub>D<sub>4</sub>. The low-temperature spectrum obtained after admitting 0.6 langmuir of C<sub>2</sub>H<sub>4</sub> to an O-rich surface with <sup>18</sup>O-cus is completely identical to the one presented in Figure 5, spectrum d (<sup>16</sup>O-cus + C<sub>2</sub>H<sub>4</sub>), with the exception that the Ru–O<sub>cus</sub> vibration signal is shifted from 103 to 99 meV. However, when comparing spectrum a (<sup>16</sup>O-cus + C<sub>2</sub>H<sub>4</sub>, 250 K) and spectrum b (<sup>18</sup>O-cus + C<sub>2</sub>H<sub>4</sub>, 250 K) in Figure 10, we realize that the peaks at 109, 125–128, 144, and 170 meV remain unaffected, whereas the signals at 164 and 211 meV shift to 159.5 and 207 meV, respectively. This points to an assignment of the latter signals to vibrations associated with O–C groups, supported by the expected isotope shift of 1.02. This assignment is further confirmed by the fact that spectrum c (<sup>16</sup>O-cus + C<sub>2</sub>D<sub>4</sub> at 250 K) again shows signals at 161 and 207 meV in agreement with the isotope shift. (Both <sup>18</sup>O and D shift the respective O–C vibrational mode.) The C–O related signal at 211/207/207 meV is assigned to a double-bond C–O group and the other C–O-related signal at 164/159.5/161 meV to a single-bond C–O group.

Looking in more detail to the temperature dependence, we found out that the reaction occurs around 200 K. The fingerprints of the reaction at 200 K can be summarized as follows:

(1) The bonding configuration of ethylene changed from  $\pi$ - to  $\sigma$ -type. There are several indications for this change in the HREEL spectra: (a) The C=C vibration at 194 (180 for C<sub>2</sub>D<sub>4</sub>) meV disappears, (b) a new C–C single bond vibration appears at 144 (136 for C<sub>2</sub>D<sub>4</sub>) meV supported by the isotope shift of



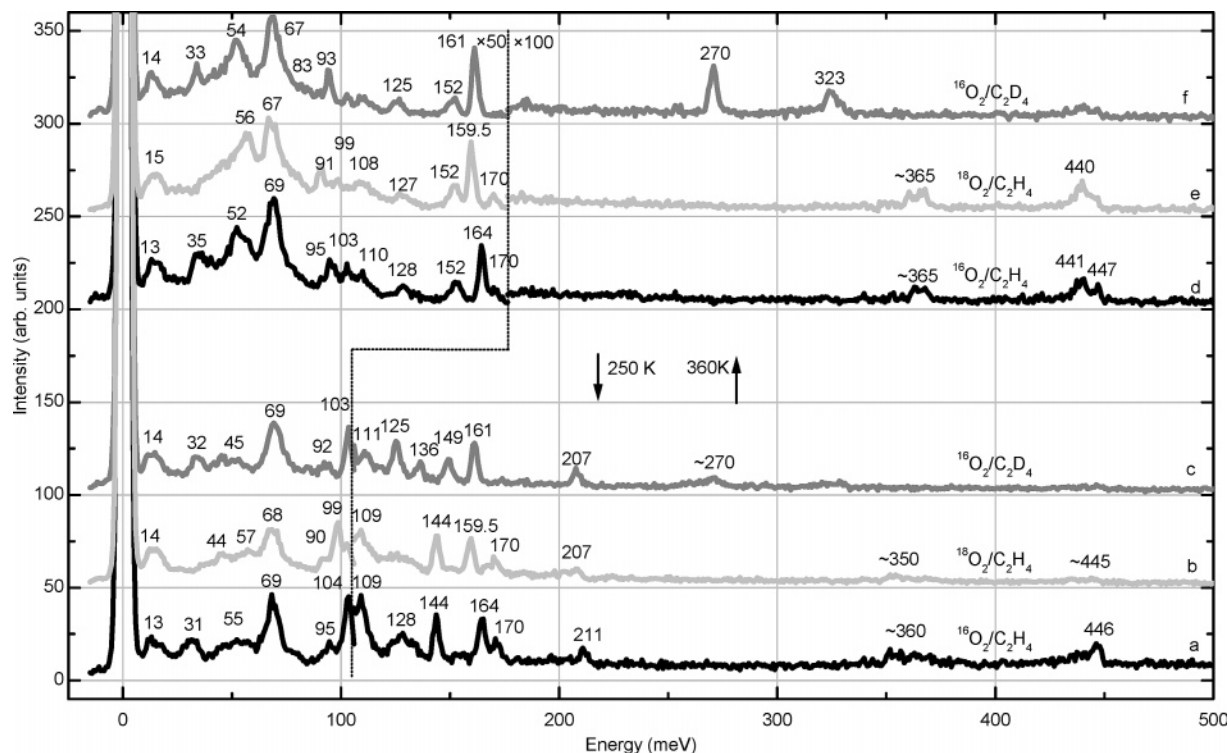


**Figure 10.** HREEL spectra recorded at 85 K after preparing an oxygen-rich  $\text{RuO}_2(110)$  surface with 1.0 langmuir of  $^{16}\text{O}_2$  or  $^{18}\text{O}_2$ , and exposing 0.6 langmuir of  $\text{C}_2\text{H}_4$  or  $\text{C}_2\text{D}_4$  at 85 K and heating to 250 K (a–c) and 360 K (d–f), respectively. Key: (a)  $^{16}\text{O}_2/\text{C}_2\text{H}_4/250$  K; (b)  $^{18}\text{O}_2/\text{C}_2\text{H}_4/250$  K; (c)  $^{16}\text{O}_2/\text{C}_2\text{D}_4/250$  K; (d)  $^{16}\text{O}_2/\text{C}_2\text{H}_4/360$  K; (e)  $^{18}\text{O}_2/\text{C}_2\text{H}_4/360$  K; (f)  $^{16}\text{O}_2/\text{C}_2\text{D}_4/360$  K.

1.06, and (c) the C–H modes shift to lower energy. These changes were also observed for the stoichiometric surface.

(2) The characteristic O-cus vibration at 104/99/103 meV in spectra a–c of Figure 10, respectively, is strongly reduced in intensity. This correlates with the next two observations.

(3) Most importantly, new bands appear at 211/207/207 meV. This is just the energy range expected for  $\text{C}=\text{O}$  groups.

(4) There is a new loss at 164/159.5/161 meV, an energy typical for a  $\text{C}-\text{O}$  single bond.

(5) C–H modes are still observed shifting from 372/384 (278/288) to 350–360 (270) meV in agreement with the change from  $\pi$ - to  $\sigma$ -bonding.

(6)  $\text{H}_2\text{O}$  shows up at 55, 95, 109, 128, and 446 meV, a set of energies quite typical for  $\text{H}_2\text{O}_{\text{cus}}$ , especially, since the loss at 230 meV, typical for  $\text{H}_2\text{O}_{\text{bridge}}$ , is missing.<sup>10</sup>

(7) The wagging etc. modes are hard to discriminate any longer.

From these results we conclude that O-cus is reactively consumed by the rehybridized ethylene which establishes direct bonds to O-cus.

**3.2.3. Model for the  $\text{C}_2\text{H}_4-\text{O}_{\text{cus}}$  Reaction at 200 K.** From the experimental findings presented above we tentatively set up a model for the first reaction step(s) between  $\text{C}_2\text{H}_4$   $\pi$ -bonded to Ru-cus and O-cus as shown schematically in Figure 11. The basic element is a single Ru-cus site between two O-cus species as the active site. Figure 11a shows  $\pi$ -bonded  $\text{C}_2\text{H}_4$  between O-cus neighbors. At about 250 K,  $\pi$ -bonded  $\text{C}_2\text{H}_4$  has changed to  $\sigma$ -bonded  $\text{C}_2\text{H}_4$  which interacts with O-cus to form  $\text{O}-\text{C}-\text{C}$  bridging complexes exhibiting  $\text{C}-\text{O}$  single and double bonds, respectively, similarly as suggested by Linic et al.<sup>20</sup> We know that O-cus is acting as an acceptor for the split-off H atoms resulting in  $\text{H}_2\text{O}_{\text{cus}}$  which desorbs at 400 K. Because of the relatively large separation of 3.11 Å between two nearest neighbor Ru-cus atoms a direct interaction between the bonding C atom and O-cus leading to an  $\eta_1(\text{O})$  or  $\eta_2(\text{C},\text{O})\text{CH}_3\text{CHO}$

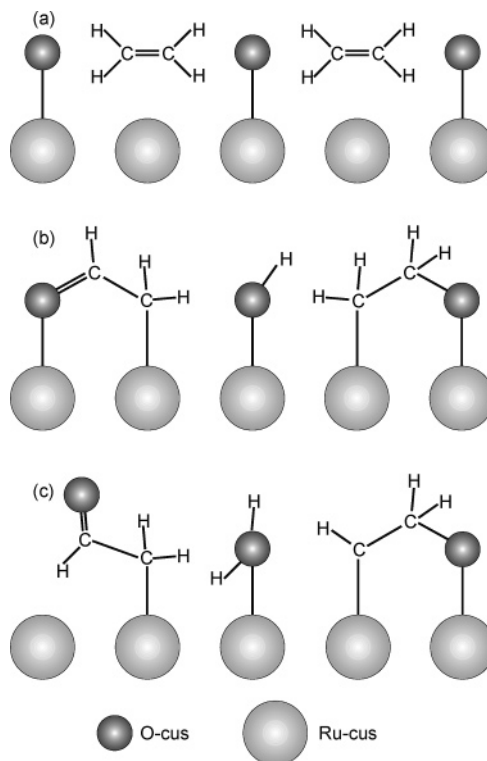


**Figure 11.** Schematic overview of different surface species possible as intermediates upon interaction of ethylene with Ru-cus and O-cus: (a)  $\pi$ -bonded  $\text{C}_2\text{H}_4$ ; (b)  $\sigma$ -bonded  $\text{C}_2\text{H}_4$  with one  $\text{C}=\text{O}$  double bond (left-hand side), one  $\text{C}-\text{O}$  single bond (right-hand side), and one  $\text{HO}_{\text{cus}}$ ; (c)  $\sigma$ -bonded  $\text{C}_2\text{H}_4$  with one  $\text{C}=\text{O}$  double bond (left-hand side), one  $\text{C}-\text{O}$  single bond (right-hand side), and one  $\text{H}_2\text{O}_{\text{cus}}$ . Geometric interatomic distances in the drawing correspond approximately to bond lengths (for further details see text).

complex<sup>13</sup> is highly improbable. Instead, we propose that the C group of  $\sigma$ -bonded  $\text{C}_2\text{H}_4$ , which is not fixed to Ru-cus, interacts



with the neighboring O-cus starting a reaction sequence of  $\text{C-H}$  to  $\text{-C-O}$  to  $\text{-C=O}$  such as illustrated in Figure 11, parts b and c. After a split-off of H, the  $\text{C-O}$  bond in the  $\text{-C-O-Ru}$  chain may be strengthened leading to the formation of a  $\text{C=O}$  double bond and a breaking of the  $\text{O-Ru}$  bond (see Figure 11c left side). Our HREEL spectra indicate that at 250 K we have a coexistence of  $\text{-C-C-Ru}$  and  $\text{-C=O}$  configurations. The  $\text{C-O}$  stretch of the double bond measured at 211 meV ( $\text{C}_2\text{H}_4$ ) is higher than the 208 meV reported for  $\eta_1(\text{O})\text{CH}_3\text{CHO}$  on  $\text{Ru}(0001)$ ,<sup>13</sup> but smaller than 217 meV for gaseous  $\text{CH}_3\text{CHO}$ . This difference is in further support of a missing oxygen-surface bond, such as present for adsorbed  $\eta_1(\text{O})\text{CH}_3\text{CHO}$ . However, the vibrational frequencies of the species in Figure 11b are presumably quite similar to those of adsorbed  $\eta_2(\text{O})\text{CH}_3\text{CHO}$ . Considering the models in Figure 11, one should keep in mind, however, that the real situation is three-dimensional whereas only one plane normal to the surface is considered in the Figure.

**3.2.4. Thermal Activation up to 500 K for  $\text{C}_2\text{H}_4$  on O-rich RuO<sub>2</sub>(110).** When the sample was heated to 360 K (Figure 10, spectra d–f) further spectral changes occur. Most importantly, the signal assigned to the  $\text{C-C}$  stretch vibration at 144 meV vanishes completely, indicating the complete fragmentation of ethylene. Furthermore, the signal of  $\text{-C=O}$  at 211(207) meV is no longer visible, also indicating a further change in the C containing surface groups.

On the other hand, the signals due to  $\text{C-O}$  single bonds at 164(159.5, 161) meV are among the strongest in the spectra. In the  $\text{C}_2\text{D}_4$  spectrum f, only a single  $\text{C-D}$ -stretch vibration is observed at 270 meV, indicating that only CD groups with one single D are left at the surface. In the case of the  $\text{C}_2\text{H}_4$  spectra it is not quite clear, whether there are still two vibrational signals or only one broad vibrational band at  $\sim 365$  meV. Simultaneously, the signals corresponding to the  $\text{H}_2\text{O}_{\text{cus}}$  groups at 52, 95, 110, and 441 meV gain intensity (spectra d and e) because 360 K lies below the  $\text{H}_2\text{O}_{\text{cus}}$  desorption temperature of 400 K.

Warming to 450 K does not lead to a new situation. At this temperature,  $\text{H}_2\text{O}_{\text{cus}}$  has already left the surface and one may expect new intermediates to be formed. This is not the case, instead a whole sequence of final reaction steps seem to proceed just around 500 K at which temperature the final  $\text{H}_2\text{O}$  and  $\text{CO}_2$  reaction products are desorbing.

When the sample is heated further to 500 K (not shown), i.e., to the formation temperature of  $\text{CO}_2$ , the spectra look nearly identical to the ones observed after heating to 400 K in the case of the stoichiometric surface (Figure 6, spectra c and d). Signals at 448 meV (330 meV) are attributed to OH- (OD-) bridge which later desorb as  $\text{H}_2\text{O}_{\text{bridge}}$  after disproportionation in the temperature range between 500 and 700 K (compare Figure 8). There is a remaining signal at 152 meV due to  $\text{O-C}$  vibrations of some remaining C fragments. When the sample is heated to even higher temperatures, the stoichiometric  $\text{RuO}_2(110)$  surface is completely restored.

Finally we note that a lower density of O-cus atoms at the starting surface does not enhance the reaction rate, instead leads to a partial desorption of unreacted  $\text{C}_2\text{H}_4$ . This was studied in detail for a  $\text{RuO}_2(110)$  surface enriched with only 60% of O-cus through an exposure of 0.4 langmuir of  $\text{O}_2$ . This finding means that for reaction  $\text{C}_2\text{H}_4$  needs a close neighborhood of O-cus atoms, i.e., the reaction occurs most likely with an ethylene molecule at a single empty Ru-cus site between two O-cus atoms.

In summary, when an oxygen-saturated  $\text{RuO}_2(110)$  surface is exposed to ethylene at 85 K, the molecule is  $\pi$ -bonded to a

Ru-cus atom. When annealed at 200 K, a complex interaction of the adsorbed ethylene with O-cus is observed, accompanied by a change to  $\sigma$ -bonding and partial dehydrogenation, leading to  $\text{H}_2\text{O}_{\text{cus}}$ —which desorbs later at 400 K—as well as two types of  $\text{-C-O}$  groups within the fragments. When the temperature is increased to 360 K, further dehydrogenation of ethylene takes place accompanied by  $\text{C-C}$  bond rupture and interaction of the  $\text{CH}_x$  fragments with O-bridge and O-cus. Around 500 K, the dehydrogenation is complete and the  $\text{CO}$  intermediate reacts with an additional O atom to form  $\text{CO}_2$ , which desorbs immediately accompanied by  $\text{H}_2\text{O}_{\text{bridge}}$  and  $\text{H}_2$ . Another  $\text{H}_2\text{O}_{\text{bridge}}$  surface group releases hydrogen in forming  $\text{O}_{\text{bridge}}\text{H}$  and desorbs between 500 and 700 K as  $\text{H}_2\text{O}$ . Between 360 and 500 K no further surface groups are observed. Therefore, at 500 K a whole sequence of correlated reaction steps seem to occur which leads finally to the desorption of the  $\text{CO}_2$  and  $\text{H}_2\text{O}$  reaction products. Different reaction steps are not resolvable in time by our methods.

Formation of ethylene oxide is not observed, neither as a surface intermediate nor as a desorption product. One may rationalize this as follows: The O-cus atoms seem to be too localized and protrude too much out of the surface so that a  $\text{C}_2\text{H}_4$  molecule can be aligned nearby in order to insert the O atom into the double bond. There is no nearby bonding of the  $\text{C}_2\text{H}_4$  to be held strongly enough at the surface to allow this reaction step.

#### 4. Conclusion

We investigated the interaction of ethylene with the stoichiometric and the oxygen-rich  $\text{RuO}_2(110)$  surface. While the thermal stability of the various surface species was probed by TDS, HREELS experiments provided information about their vibrational signals and the formation of reaction intermediates. At 85 K ethylene is adsorbed molecularly in a  $\pi$ -bonded configuration on both surfaces on empty Ru-cus sites. For adsorption on the stoichiometric surface, a  $\text{C}_2\text{H}_4$  saturation coverage is reached at an exposure of 1.0 langmuir. When the sample is heated to 260 K, a transition from  $\pi$ -bonded to  $\sigma$ -bonded ethylene occurs. Desorption is completed around 320 K.

Following ethylene adsorption on the oxygen-rich surface, the first couple of reactions are observed at 200 K taking place on Ru-cus: a change from  $\pi$ - to  $\sigma$ -bonding, formation of  $\text{-C=O}$  and  $\text{-C-O}$  groups, and dehydrogenation giving rise to  $\text{H}_2\text{O}$  adsorbed at Ru-cus.  $\text{H}_2\text{O}_{\text{cus}}$  leaves the surface later at the typical temperature of 400 K. The maximum reaction rate is reached for  $\text{C}_2\text{H}_4$  chemisorbed at Ru-cus with O-cus neighbors on each side. For O-cus coverage lower than the saturation value of about 80%, the reaction rate is not increased, but molecular  $\text{C}_2\text{H}_4$  desorption occurs along with combustion. A model for this first couple of reactions is sketched. Also, a final interaction with O-bridge is concluded. A reaction with both O-cus and O-bridge is reasonable because a single  $\text{C}_2\text{H}_4$  consumes two O-bridge besides the four O-cus atoms. The final products of ethylene combustion ( $\text{CO}_2$ ,  $\text{H}_2\text{O}_{\text{bridge}}$ ) are forming and desorbing at 500 K in a very narrow time window which is not resolvable with our methods. Ethylene oxide is not detected under any circumstance. It is argued that O-cus protrudes too much out of the surface to align a  $\text{C}_2\text{H}_4$  molecule nearby in order to insert the O-cus into the double bond.

**Acknowledgment.** We acknowledge skillful technical support by P. Geng and valuable assistance by M. Richard in editing the manuscript.

## References and Notes

- (1) van Santen, R. A.; Kuipers, H. P. C. E. *Adv. Catal.* **1987**, 35, 265.
- (2) Fan, C. Y.; Wang, J.; Jacobi, K.; Ertl, G. *J. Chem. Phys.* **2001**, 114, 10058.
- (3) Wang, J.; Fan, C. Y.; Jacobi, K.; Ertl, G. *J. Phys. Chem. B* **2002**, 106, 3422.
- (4) Kim, Y. D.; Seitsonen, A. P.; Wendt, S.; Wang, J.; Fan, C.; Jacobi, K.; Over, H.; Ertl, G. *J. Phys. Chem. B* **2001**, 105, 3752.
- (5) Over, H.; Kim, Y. D.; Seitsonen, A. P.; Wendt, S.; Lundgren, E.; Schmid, M.; Varga, P.; Morgante, A.; Ertl, G. *Science* **2000**, 287, 1474.
- (6) Lafosse, A.; Wang, Y.; Jacobi, K. *J. Chem. Phys.* **2002**, 117, 2823.
- (7) Wang, J.; Fan, C. Y.; Jacobi, K.; Ertl, G. *Surf. Sci.* **2001**, 481, 113.
- (8) Wang, Y.; Lafosse, A.; Jacobi, K. *J. Phys. Chem. B* **2002**, 106, 5476.
- (9) Lambert, R. M.; Ormerod, R. M.; Tyspe, W. T. *Langmuir* **1994**, 10, 730.
- (10) Wang, J.; Fan, C. Y.; Sun, Q.; Reuter, K.; Jacobi, K.; Scheffler, M.; Ertl, G. *Angew. Chem. Int. Ed.* **2003**, 42, 2151.
- (11) Paulus, U. A.; Wang, Y.; Bonzel, H. P.; Jacobi, K.; Ertl, G. To be published.
- (12) Hills, M. M.; Parmeter, J. E.; Mullins, C. B.; Weinberg, W. H. J. *Am. Chem. Soc.* **1986**, 108, 3554.
- (13) Henderson, M. A.; Mitchell, G. E.; White, J. M. *Surf. Sci.* **1988**, 203, 378.
- (14) Bent, B. E.; Mate, C. M.; Kao, C.-T.; Slavin, A. J.; Somorjai, G. A. *J. Phys. Chem.* **1988**, 92, 4720.
- (15) Stuve, E. M.; Madix, R. J. *J. Phys. Chem.* **1985**, 89, 3183.
- (16) Kim, S. H.; Paulus, U. A.; Wang, Y.; Winterlin, J.; Jacobi, K.; Ertl, G. *J. Chem. Phys.* **2003**, 119, 9729.
- (17) Stacchiola, D.; Burkholder, L.; Tyspe, W. T. *Surf. Sci.* **2002**, 511, 215.
- (18) Steininger, H.; Ibach, H.; Lehwald, S. *Surf. Sci.* **1982**, 117, 685.
- (19) Lobo, A.; Conrad, H. *Surf. Sci.* **2003**, 523, 279.
- (20) Linic, S.; Medlin, J. W.; Barteau, M. A. *Langmuir* **2002**, 18, 5197.